Simulation of Adsorption Isotherms of Water on Ionic Surfaces[$]

Elmar Stöckelmann*, Ewald Mirko Aydt and Reinhard Hentschke

Max-Planck-Institut für Polymerforschung, Postfach 3148, 55021 Mainz, Germany (stoeckel@mpip-mainz.mpg.de)

Abstract

The intention of this work is to aid the construction of a water model capable of describing bulk water in contact with ionic surfaces. The model should be sufficiently simple to be useful for simulating large systems. Here, the extended simple point charge (SPC/E) water model, which is one of the most commonly used descriptions of bulk water, was tested in a strongly heterogeneous system. Simulations were carried out on the NaCl(100) and the calcite($10\bar{1}4$) surfaces, described in terms of Lennard-Jones and Coulomb potentials. On the NaCl surface Molecular Dynamics simulations show that SPC/E water forms clusters due to its high permanent dipole moment. Better agreement with the experimental adsorbate structure was achieved by reducing the water dipole moment to its gas phase value. On the calcite surface adsorption isotherms were simulated using a Molecular Dynamics-Monte Carlo hybrid technique, which consists of a normal Molecular Dynamic simulation with randomly chosen insertion and removal Monte Carlo steps repeated after a constant time period. The method is tested by calculating adsorption isotherms for two Lennard-Jones systems, i.e. methane in contact with the graphite basal plane and with the zeolite silicalite (ZSM5), for which we obtain excellent agreement with the experimental isotherms. For calcite, however, the simulated adsorption isotherms again show a strong dependence on the choice of the dipole moment. The SPC/E value yields a strongly exaggerated coverage, whereas the gas phase value severely underestimates the coverage in comparison with the experiment. From our results we draw the conclusion that a fixed charged model is not recommendable for the simulation on ionic surfaces, and that it is highly desirable to include variable polarization.

Keywords: Molecular dynamics, Monte Carlo, adsorption, water, sodium chloride, calcium carbonate

Introduction

Computer simulations of molecular adsorption from the gas or from the liquid phase onto solid surfaces are subject to two mutually limiting requirements. On the one hand, the Hamiltonian of the system has to be sufficiently accurate to describe the delicate interplay between the substrate-adsorbate and the adsorbate-adsorbate interactions. On the other hand, the system has to be large enough to minimize boundary induced frustration of the equilibrium adsorbate structure while allowing time scales long enough to model the surface induced ordering phenomena of interest. Thus, empirical force field simulations utilizing Molecular Dynamics (MD) and Monte Carlo (MC) techniques are frequently the method of choice in the case of physisorption [1,2]. A key challenge in empirical force field modeling, however, is the

[$] *Presented at the 11. Molecular Modeling Workshop, 6 -7 May 1997, Darmstadt, Germany*

* *To whom correspondence should be addressed*

transferability of the model potentials. Preferably the potentials should perform equally well in different bulk phases as well as in heterogeneous systems and over a wide range of values of the thermodynamic variables. Liquid/solid or gas/solid interfaces encompass all of these aspects due to the inherent anisotropy of the system manifested in large spatial density and/or electric field variations near the solid surface. A system which is particularly interesting in this context is water on ionic surfaces. Aqueous surface environments are of great technical importance, and, in addition, there is a long history of optimizing empirical water models in the bulk.

In this work we investigate the interaction of the perhaps most frequently used fixed charge water model, i.e. the SPC/E model [3], with two ionic substrates, NaCl(100) and calcite ($10\bar{1}4$). In the case of NaCl(100) we study the temperature dependent monolayer structure, whereas in the case of calcite ($10\bar{1}4$) we focus on the adsorption isotherm. The latter quantity is particularly useful for testing the interaction potentials, because it encompasses both the pure adsorbate-substrate interactions at low coverages as well as the additional adsorbate-adsorbate interactions at higher coverages. Adsorption isotherms in the low coverage or low gas pressure limit are most suitably simulated using grand canonical techniques [1]. This is because the chemical potential of the gas phase is easily related to the pressure via the ideal gas law or a low order virial expansion. At high gas pressure, where the chemical potential is not so readily available, the simulation of the full system, i.e. the surface in equilibrium with the bulk phase is more appropriate [4]. Here we employ both classical Molecular Dynamics simulations and a hybrid Molecular Dynamics-Monte Carlo method (MCMD) similar to those in [5,6]. First we test our MCMD algorithm simulating adsorption isotherms of methane interacting with the basal plane of graphite and with the zeolite silicalite (ZSM5). In both cases we find excellent agreement with the experiment. Subsequently we simulate water on NaCl at fixed coverage using normal MD and on calcite using the MCMD algorithm. The main conclusion of these water simulations is that even though the simulation techniques can be shown to work well for the test systems there are significant discrepancies between the simulation results and the experiment in the case of the aqueous systems. We show that these discrepancies are most likely due to the neglect of dynamically induced polarization.

Method

Interaction potentials

Empirical potential functions U of molecular systems usually are comprised of two parts, i.e., $U = U_{valence} + U_{nonbond}$. The valence part, $U_{valence}$, describes the bonded intramolecular interactions, whereas the non-bonded part, $U_{nonbond}$, models longer-ranged atomic interactions within and between molecules. In the present work, as will become clear below, we do not need $U_{valence}$ and the intramolecular contributions to

$U_{nonbond}$ explicitly. For the remainder of $U_{nonbond}$ we make the simplifying assumption that pairwise Lennard-Jones and Coulomb interactions are sufficient to describe both adsorbate-adsorbate and adsorbate-substrate interactions. Thus, the potential energy of the adsorbate is

$$U = \sum_{i<j} \left\{ \varepsilon_{ij} \left[\left(\frac{\sigma_{ij}^*}{r_{ij}}\right)^{12} - 2\left(\frac{\sigma_{ij}^*}{r_{ij}}\right)^6 \right] + \frac{q_i q_j}{r_{uj}} \right\} \\ + \sum_i u_i^{sub}(\vec{r}_i) \tag{1}$$

and

$$u_i^{sub}(\vec{r}_i) = \sum_k \left\{ \varepsilon_{ij} \left[\left(\frac{\sigma_{ik}^*}{r_{ik}}\right)^{12} - 2\left(\frac{\sigma_{ik}^*}{r_{ik}}\right)^6 \right] + \frac{q_i q_k}{r_{ik}} \right\} \tag{2}$$

Here $r_{ij} = |\vec{r}_i - \vec{r}_j|$ is the distance between two adsorbate sites, and $r_{ik} = |\vec{r}_i - \vec{r}_k|$ is the distance between an adsorbate atom i and a substrate atom k. ε and σ^* are the corresponding Lennard-Jones parameters (Note that σ^* is the position of the minimum.), and the q are partial charges located on the interaction sites. Notice also that there are no intra-substrate interaction terms, because the substrate is assumed to be rigid.

In the case of the short-ranged Lennard-Jones interactions the summations over k can be performed directly. However, for sufficiently smooth substrate surfaces or if the range of the adsorbate-substrate interactions is long a different approach becomes advantageous (e.g., [2]). The substrate is decomposed into a stack of identical layer planes l. Subsequently, the interactions between an adsorbate atom and the atoms in each layer plane are carried out on the layer plane's reciprocal lattice characterized by lattice vectors $\vec{g}$. The result can be written as

$$u_i^{sub}(\vec{r}_i) = \sum_l u_l^{(o)}(z_{li}) + \sum_{l,\vec{g}\neq 0} u_l^{(g)}(z_{li}, \vec{\tau}_{li}),$$

where $g = |\vec{g}|$. Note that the first term depends only on the perpendicular separation between the adsorbate atom and the lth layer plane, z_{li}, whereas the second term depends also on the lateral position of i relative to the lth plane, $\vec{\tau}_{li} = (x_{li}, y_{li})$, i.e. on the corrugation of the surface. This latter term decays exponentially with increasing z_{li}. In the case of the methane-graphite interaction considered below u_i^{sub} to good approximation is given by $u_0^{(o)}$, i.e.

$$u_i^{sub(I,J)}\left(\vec{r}_i\right) = \pi n_{sub}\varepsilon'_{ik}\sigma'^{*2}_{ik}\left[\frac{1}{5}\left(\frac{\sigma'^*_{ik}}{z_i}\right)^{10} - \left(\frac{\sigma'^*_{ik}}{z_i}\right)^4\right] \qquad (3)$$

where $z_i = z_{0i}$, and $n_{sub} = 0.382$ Å^{-2} is the atom density in the basal plane. Note that the methane molecule is modeled as a united atom with one set of effective Lennard-Jones parameters. The primes in (3) indicate that the parameters are adjusted relative to the original atom-atom parameters to account for the neglect of the lower lying layers (The parameters in table 1 are the primed parameters). For the longer-ranged Coulomb interactions the full surface potential is used, which is given by

$$u_i^{sub(Coulomb)}\left(\vec{r}_i\right) =$$
$$q_i\frac{2\pi}{A_s}\sum_l q_l\sum_{\vec{g}\neq 0} e^{i\left[g_x\left(x_{li}-x_l^q\right)+g_y\left(y_{li}-y_l^q\right)\right]}\frac{e^{-gz_{li}}}{g} \qquad (4)$$

Here A_s is the area of the layer unit cell which contains one partial charge q_l. The x_l^q and y_l^q are the coordinates of q_l relative to the layer plane. Note that $\vec{g} = 0$ is excluded from the sum, which essentially is a consequence of neutrality and stability conditions fulfilled by the crystal. Otherwise the summations in (4) are evaluated to the limit of numerical accuracy.

Simulation techniques

The adsorption isotherms calculated in this work are simulated using a grand canonical ensemble generated via a combination of Molecular Dynamics and Monte Carlo steps. However, here the molecules are not inserted continuously into the system [5], but rather instantaneously similar to [6]. The spatial displacement of the molecules follows Newton's equation of motion, $\ddot{\vec{r}}_i = -\frac{1}{m_i}\vec{\nabla}_i U$, which are integrated using the leapfrog Verlet schema combined with the SHAKE bond-length constraint algorithm [7] (for water) and a Berendsen thermostat [8]. After a certain period Δt_{mc} both an insertion and a removal trial are performed using a symmetrical algorithm often referred to as Barker sampling [1]. A new molecule is inserted subject to the condition

$$\left[1 + \frac{N+1}{aV}\exp\left(\frac{\Delta U_{insert}}{k_B T}\right)\right]^{-1} \geq \xi \qquad \xi \in N[0,1] \qquad (5)$$

where N is the number of molecules in the volume V, and an existing one is removed according to

$$\left[1 + \frac{aV}{N}\exp\left(\frac{\Delta U_{remove}}{k_B T}\right)\right]^{-1} \geq \xi \qquad \xi \in N[0,1] \qquad (6)$$

$\Delta U_{insert} = U(N+1)-U(N)$ and $\Delta U_{remove} = U(N-1)-U(N)$ are the respective changes of the potential energy due to the insertion and the removal of one molecule. The position of the inserted molecule is randomly chosen within V, and the velocity of its centre of mass is assigned according to a Maxwell-Boltzmann distribution for the selected temperature, T. Note that no rotational energy is assigned to the inserted molecule. The activity, a, in (5) and (6) is related to the chemical potential, μ, and to the bulk pressure, P, via

$$a = \frac{1}{\Lambda^3}\exp\left(\frac{\mu}{k_B T}\right) \qquad (7)$$

$$= \left(\frac{P}{k_B T}\right) + B_2(T)\left(\frac{P}{k_B T}\right)^2 + \dots \qquad (8)$$

where Λ is the generalized thermal wavelength and $B_2(T)$ is the second virial coefficient. A particular advantage of the MCMD algorithm is that it can easily be implemented in an existing Molecular Dynamics program, which in our case is part of the AMBER package version 4.1[9].

Results

Methane isotherms

In order to test the above grand canonical MCMD algorithm, e.g., the effects of the instantaneous particle insertion and the attending discontinuity in the potential and forces, we simulate the well known adsorption isotherms of methane on the graphite basal plane and in the zeolite silicalite (ZSM5). In both cases the methane-methane interactions are computed according to (1). The parameters are based on the experimental temperature dependence of the second virial coefficient [4] using a 10 Å cutoff (cf. Table 1).

In the graphite case the methane molecules are constraint between two parallel interfaces (44.28×42.6 Å^2) applying periodic boundary conditions parallel to the surfaces. Each surface interacts with methane via the potential (3), which was parameterized according to the experimental temperature dependence of the Henry's constant [4]. Note that the surface-to-surface separation, L, is large, i.e. $L = 100$ Å, so that bulk conditions are maintained in the central region between the surfaces.

Figure 1 illustrates the time evolution of the number of methane molecules between the surfaces, N, for given values of a and T as a function of Δt_{mc}, the time between two re-

moval/insertion attempts. For long times t there appears to be no effect on N for the range of Δt_{mc}-values investigated here. A smaller Δt_{mc}, however, shortens the time necessary for attaining the plateau, but it is recommendable to use a period which is sufficiently large in order to not disturb the equilibrium structure of the gas in the bulk or near the surface. In the following we use $\Delta t_{mc} = 250$fs and a MD time step of 1fs. Figure 1 also illustrates that the choice of the initial number of particles $N(t=0)$ has no influence on the long time plateau. Nevertheless, starting with $N(t=0)=0$ has the advantage, that it is not necessary to construct an initial molecular configuration.

Figure 2 shows the simulated surface excess concentration, $\Gamma^\sigma = \int_{z'}^{\infty} [\rho(z) - \rho_{bulk}]dz$, as a function of the bulk pressure, P. Here $\rho(z)$ is the gas density at distance z from the surface, and z' is defined as the onset of $\rho(z)$. Both P and the bulk density, ρ_{bulk}, are related to the activity, a, via $P=k_BT\,a$ $(1-B_2a)$ (cf. eqn. (8); for the range of pressures considered here the contribution due to the third virial coefficient is less than 0.5%), and $\rho_{bulk}=a(1-2\,B_2a)$ with $B_2(323\,K)= -5\text{Å}^3$ and $B_2(253\,K) = -90\text{Å}^3$ (theoretical values based on ε and σ^* used in reference 4). Here the MCMD calculations are carried out at low pressures ranging from 1 to 50 bar, and there is good agreement between the simulations and the experimental isotherms [10]. The figure also includes the simulation results of a previous MD simulation with constant N [4]. In this case P was determined via the density in the centre of the slit, $\rho_{L/2}$, at fixed surface separation, relating the two quantities through an independent simulation at $\rho_{L/2}$ in the ab-
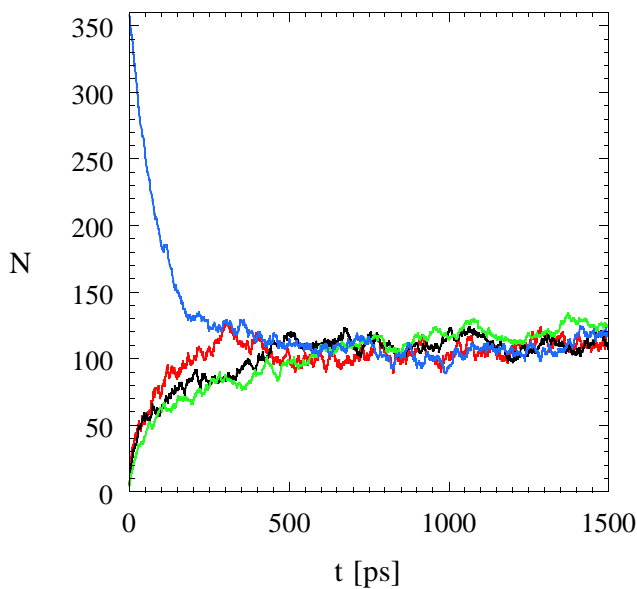
Table 1. *Lennard-Jones parameters and charges*

Lennard-Jones methane parameters:

		σ^* [Å]	ε/k_B [K]
Me	Me	4.254	148.7[4]
Me	$C_{graphite}$	4.4(σ'^*)	72.17 (ε'^*) [4]
Me	$O_{zeolite}$	3.214	132.3 [13]

Lennard-Jones water-water interaction parameters:

		σ^* [Å]	ε/k_B [K]
O_{H_2O}	O_{H_2O}	3.5532	78.2 [3]

Charges

H$_2$O gas phase	$q_H = 0.3336e$	$q_O = -0.6672e$
H$_2$O bulk	$q_H = 0.4238e$	$q_O = -0.8476e$
Ca^{2+}	$q_{Ca} = 2e$	
CO$_3^{2-}$	$q_C = 0.9193e$	$q_O = -0.9731e$
Na$^+$	$q_{Na} = 1e$	
Cl$^-$	$q_{Cl} = -1e$	

Surface interaction parameters of the original SPC/E water (dipole moment $\mu = 2.35$ D)

		σ^* [Å]	ε/k_B [K]
O_{H_2O}	Ca	3.77	7.216 [19]
O_{H_2O}	$O_{CO_3^{2-}}$	3.37	153.9 [19]
O_{H_2O}	$C_{CO_3^{2-}}$	3.58	86.5 [19]
O_{H_2O}	Na	3.20	24.0 [20]
O_{H_2O}	Cl	3.75	65.0 [20]

Surface interaction parameters of gas phase water (dipole moment $\mu = 1.85$ D)

		σ^* [Å]	ε/k_B [K]
O_{H_2O}	Ca	3.4684	7.216
O_{H_2O}	$O_{CO_3^{2-}}$	3.1004	153.9
O_{H_2O}	$C_{CO_3^{2-}}$	3.2936	86.5
O_{H_2O}	Na	2.85	24
O_{H_2O}	Cl	3.75	65

Figure 1. *Time evolution of the number of molecules in the system, N, at $a = 2 \cdot 10^{-4}$ Å^{-3} and $T = 323$ K using the grand canonical MCMD algorithm. Blue curve: N(t=0)=360 and $\Delta t_{mc} = 250$ fs; red curve: N(t=0)=0 and $\Delta t_{mc} = 150$ fs; black curve: N(t=0)=0 and $\Delta t_{mc} = 250$ fs; green curve: N(t=0)=0 and $\Delta t_{mc} = 500$ fs.*

sence of surfaces. As can be seen, normal MD works quite well at high pressure, where it has the additional advantage that the chemical potential does not enter explicitly (This difficulty of grand canonical MC of course can be overcome using the Gibbs-Ensemble technique [11]). At low pressures MD becomes increasingly time consuming. Here the MC moves introduce a real advantage, because of the comparatively much faster random spatial displacement.

The results for our second MCMD-test system, methane in contact with the zeolite silicalite (ZSM5), are illustrated in Figure 3. The figure shows the number of methane molecules per zeolite unit cell, N_C, plotted against the bulk pressure, *P*, related to the activity, *a*, using $B_2(298 \text{ K}) = -60 \text{ Å}^{-3}$ (cf. above). Again we find good agreement between the experimental measurement [12], our results, the MC work of Goodbody et al. [13], and the grand canonical GEMD simulation technique [14], which refers to a MD version of the Gibbs-Ensemble MC technique. Both the present work as well as the GEMD simulation use the methane-zeolite Lennard-Jones parameters of Goodbody et al. (Table 1). Note that the zeolite potential is computed according to eqn. (2) prior to the simulation on a three-dimensional grid within the unit cell. During the simulation the potential is evaluated using the stored grid values in conjunction with a tri-linear interpolation.
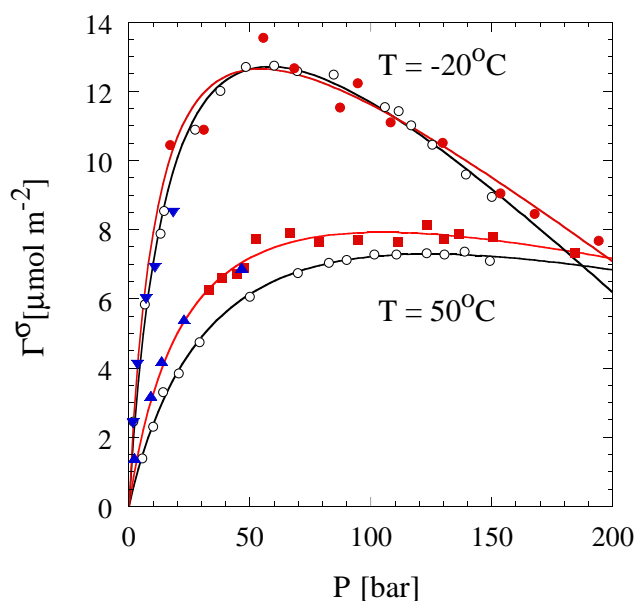
Adsorption of water on NaCl(100) and calcite (10$\bar{1}$4)

Before applying the above MCMD method to the adsorption isotherms of water on calcite (10$\bar{1}$4) we discuss the results of normal MD simulations of water adsorbed on NaCl(100) at fixed coverage. Our main motivation is to study the behaviour of one of the best and simplest fixed charge bulk water models, the three-site SPC/E model [3], in the vicinity of ionic surfaces.

SPC/E water has a rigid geometry defined by a bond length of 1 Å and a bond angle of 109.47°. All three atomic sites carry partial charges, but only the oxygen atoms interact via Lennard-Jones potentials (Table 1). Here we use molecule based cutoffs for the water-water interactions of 20 Å (for NaCl) and 16 Å (for calcite). Similar cutoffs yield good results for structural and dynamic quantities in the bulk. The interaction of water with NaCl are described by the eqns. (3) and (4). Guided by the experimental values [15] we adjust the Lennard-Jones parameters of the adsorbate-substrate interaction to obtain an isosteric heat of adsorption at zero coverage of $q_{st}^0(140 \text{ K}) = 14 \pm 1 \text{kcal/mol}$. The subsequent MD simulations are performed at monolayer coverage, i.e., 225 water molecules on a surface area of 59.7 Å × 59.7 Å, which is based on the experimental low temperature (1 × 1) superstructure [15], for different temperatures ranging from 50K to 250K. Figure 4 shows a simulation snapshot at 225 K,
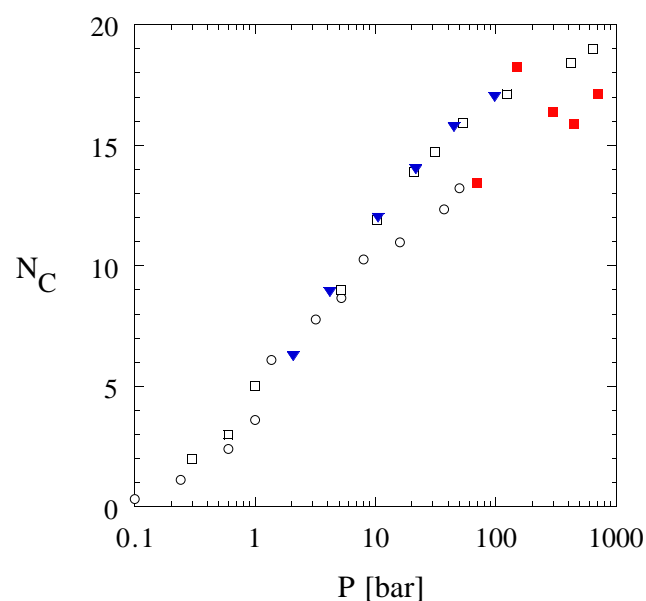

Figure 2. *Comparison of the simulated surface excess, Γ^σ, shown as a function of bulk pressure, P, with the corresponding measurements [10] for two temperatures. Hollow circles: experiment; solid blue triangles: grand canonical MCMD; solid red circles and solid red squares: MD results of reference [4]. The lines are least-squares fits through the simulation results (red) and the experimental values (black).*

Figure 3. *Adsorption of methane in the zeolite silicalite (ZSM5) at T = 298 K. Number of methane molecules per zeolite unit cell, N_C, vs. gas pressure, P. Open circles: experimental results [12]; solid blue triangles: grand canonical MCMD; solid red squares: GEMD; open squares: grand canonical Monte Carlo [13].*
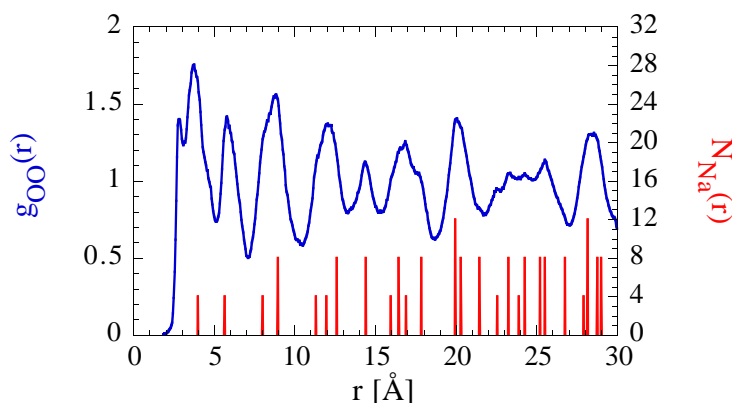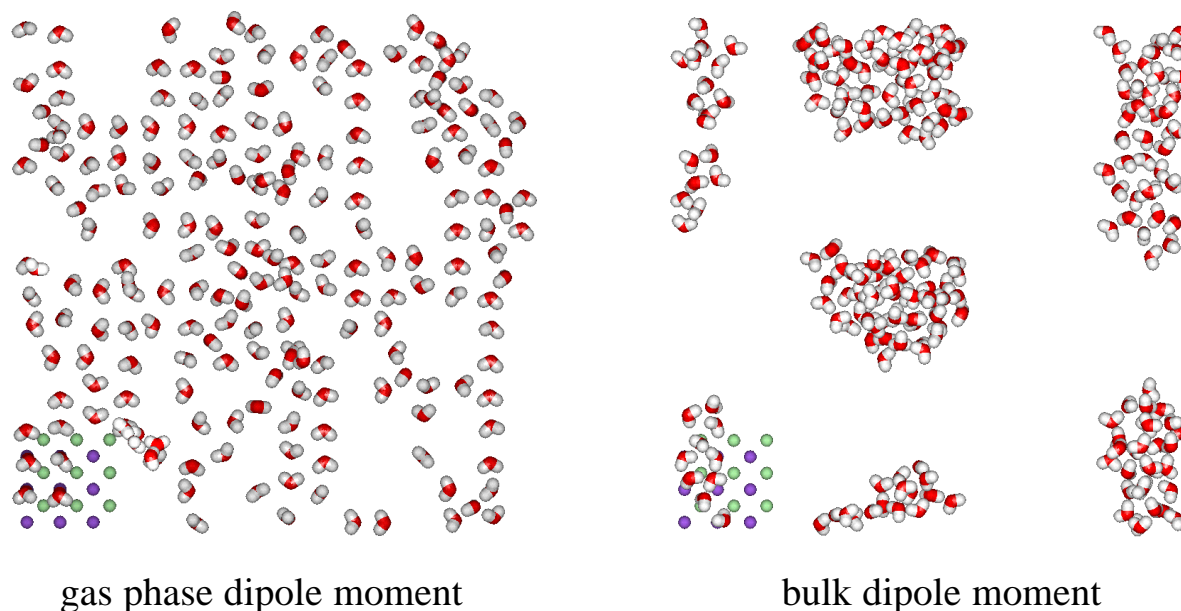
gas phase dipole moment

bulk dipole moment

Figure 4. *Top: Two simulation snapshots of water adsorbed on NaCl(100) at monolayer coverage (T = 225 K). In the lower left corners one can recognize a section of the NaCl(100) surface (purple: Na⁺; green: Cl⁻). Bottom: Oxygen-oxygen pair correlation function $g_{OO}(r)$ (blue line) for the case of the gas phase dipole moment. The vertical red lines correspond to the number of Na⁺ ions per neighbour shell of the crystal surface layer.*

where the SPC/E water molecules form clusters on the surface (right panel). At the lower temperatures the SPC/E model also does not exhibit (1 × 1) ordering but rather 'net-like' structures due to the strong dipole-dipole interaction. SPC/E water has a dipole moment of 2.35 D, which, in a mean field sense, accounts for induced polarization in the bulk liquid. In order to test the effect of the water dipole moment we carry out additional simulations using the gas phase value of 1.85 D. As a consequence of the reduced charges (cf. Table 1) we have to readjust the adsorbate-substrate Lennard-Jones

parameters according to the above value of q_{st}^0. A simulation snapshot corresponding to the one discussed above (but for the gas phase dipole moment) is shown in Figure 4 (left panel) together with the attending oxygen-oxygen pair correlation function $g_{OO}(r)$. Note that the peaks of $g_{OO}(r)$ correlate reasonably well with the positions of the sodium ion neighbour shells of the crystal surface.

The analogous comparison between the SPC/E model and its gas phase modification is also performed on calcite, where we calculate the two corresponding adsorption isotherms. The structural data for the calcite ($10\bar{1}4$) surface entering the adsorbate-substrate surface potential is used omitting relaxation, because for the ($10\bar{1}4$) surface only minor relaxation is observed in corresponding molecular mechanics calculations [16]. The first layer consists of planar CO_3^{2-} (the C-O distance is 1.282 Å) and calcium ions. The CO_3^{2-}ions are rotated around one of their C-O bonds yielding a 45° angle of the CO_3^{2-} plane relative to the surface. Each surface unit cell has an area of 8.1 Å × 5.0 Å and contains two calcium ions and two carbonate groups, allowing the adsorption of two water
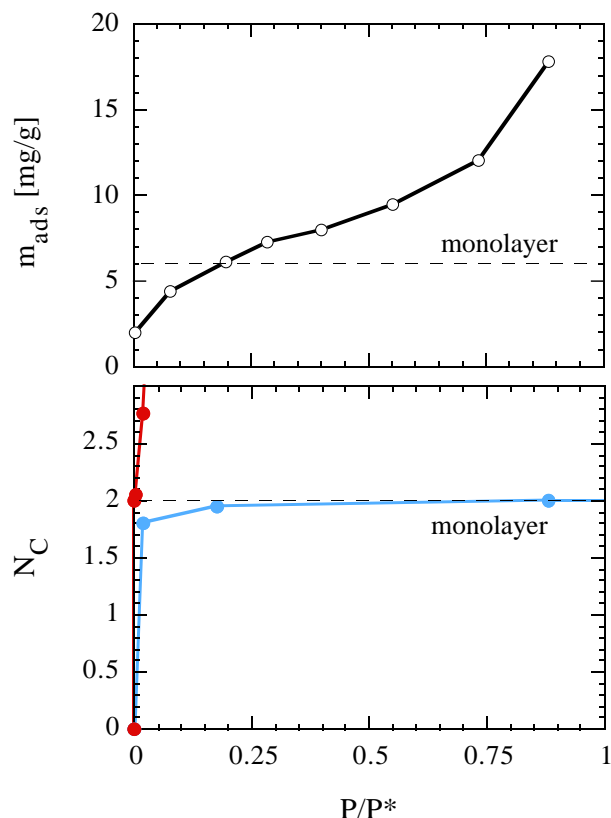
Figure 5. *Comparison of the experimental adsorption isotherm of water on precipitated calcium carbonate (upper panel) at T = 293.8 K [17] with the corresponding grand canonical MCMD isotherms of SPC/E and SPC/E-like water on calcite(10$\bar{1}$4) (lower panel). m_{ads} is the adsorbed amount of water per amount of substrate, N_C is the number of adsorbed water molecules per surface unit cell, and P* is the partial water pressure (P* = 0.023 bar at 293 K). Red circles and line: simulation using the original SPC/E charges; blue circles and line: simulation using the gas phase charges.*

molecules in the first monolayer in the vicinity of the calcium ions. As in the case of methane on graphite we employ a two-surface slit-geometry. Here each of the surfaces consisted of 28 unit cells and has a total area of 32.384 Å × 34.93 Å. The acceptance rate of insertion and removal in these simulations was found to be low. The insertion is hindered by the small number of favourable adsorption sites and the removal frequency is reduced by high energy penalty at these sites. Because of this Δt_{mc} is reduced to 15 fs (only 15 MD steps for each Monte Carlo trial). Notice, however, that the rate of successful insertions for this Δt_{mc} is even lower than in the case of methane on graphite or in silicalite. Thus, the insertion induced disturbance of the system is small.

Figure 5 shows the so obtained isotherms for the two water parameterizations as discussed for NaCl. In both cases the Lennard-Jones parameters of the water-substrate interaction are adjusted to yield $q_{st}^0 = 29 \pm 1$kcal/mol. Due to lacking experimental information q_{st}^0 is based on parameters obtained by fitting the simulated number of adsorbed water molecules (using the gas phase dipole moment) to the adsorption isotherm at a fixed pressure P/P* = 0.175. Note also that the pressure is calculated using $P = k_B T a$, which is acceptable at low pressures. Obviously however, neither of the simulated isotherms reproduces the shape of the experimental isotherm [17]. The simulations using the gas phase dipole moment predict the adsorption of only one monolayer on the surface, whereas the SPC/E model shows an exaggerated adsorption of water even at low pressures. In part this discrepancy may reflect the lacking definition of the experimental surface. However, we think that the large differences caused by the different dipole moments strongly suggests that the proper treatment of induced polarization is essential in aqueous systems near ionic surfaces. Induced polarization was included in two previous models of water on NaCl at fixed sub- and monolayer coverages [15, 18]. However, the iterative procedure used to self-consistently determine the induced dipole moments appears to be too slow to be useful for the calculation of adsorption isotherms, where long runs are necessary (typically 15 – 30 ns for H$_2$O/calcite). In addition, it is not clear that the models used in the above references do yield a consistent description of water in the dilute gas, in the bulk, and at the respective interfaces with ionic surfaces. It is this kind of transferability, however, which is desirable in order to reduce the number of adjustable parameters in a model, and thereby increase its predictive power. Calculations along this line are currently under way.

References

1. Nicholson, D.; Parsonage, N. G. *Computer Simulation and the Statistical Mechanics of Adsorption*; Academic: London, 1982.
2. Hentschke, R. *Die Makromolekulare Chemie - Theory and Simulations* **1997**, *6*, 287.
3. Berendsen, H. J. C.; Grigera, J. R.; Straatsma, T. P. *J. Phys. Chem.* **1987**, *91*, 6269.
4. Aydt, E. M.; Hentschke, R. *Ber. Bunsenges. Phys. Chem.* **1997**, *101*, 79.
5. Chagin, T.; Pettit, B. M. *Mol. Phys.* **1991**, *72*, 169.
6. Baranyai, A.; Cummings, P. T. *Mol. Sim.* **1996**, *17*, 21.
7. Ryckaert, J. P.; Ciccotti, G.; Berendsen, H. J. C. *J. Comput. Phys.* **1977**, *23*, 327.
8. Berendsen, H. J. C.; Postma, J. P. M.; van Gunsteren, W. F.; DiNola, A.; Haak, J. R. *J. Chem. Phys.* **1984**, *81*, 3684.
9. Cornell, W. D.; Cieplak, P.; Bayly, C. I.; Gould, I. R.; Merz, K. M.; Ferguson, D. M.; Spellmeyer, D. C.; Fox,

T.; Caldwell, J. W.; Kollman, P. A. *J. Am. Chem. Soc.* **1995**, *117*, 5179.

10. Specovius, J.; Findenegg, G. H. *Ber. Bunsenges. Phys. Chem.* **1978**, *82*, 174.

11. Allen, M. P.; Tildesley., D. J. *Computer Simulation of Liquids*; Oxford University: London, 1987.

12. Ding, T.; Ozawa, S.; Ogino, Y. *Zhejiang Daxue Xuebao* **1988**, 22.

13. Goodbody, S. J.; Watanabe, K.; MacGowan, D.; Walton, P. R. B.; Quirke, N. *Chem. Soc. Faraday Trans.* **1991**, *87*, 1951.

14. Hentschke, R.; Bast, T.; Aydt, E. M.; Kotelyanskii, M. *J. Mol. Model.* **1996**, *2*, 319.

15. Bruch, L. W.; Glebov, A.; Toennies, J. P.; Weiss, H. *J. Chem. Phys.* **1995**, *103*, 5109.

16. Parker, S. C.; Kelsey, E. T.; Olvier, P. M.; Titiloye, J. O. *Faraday Discuss.* **1993**, *95*, 85.

17. Ahsan, T. *Colloids and Surfaces* **1992**, *64*, 167.

18. Wassermann, B.; Mirbt, S.; Reif, J.; Zink, J. C.; Matthias, E. *J. Chem. Phys.* **1993**, *98*, 10049.

19. Teleman, O.; Ahlstrøm, P. *J. Am. Chem. Soc.* **1986**, *108*, 4333.

20. Straatsma, T. P.; Berendsen, H. J. C. *J. Chem. Phys.* **1988**, *89*, 5876.